Monatshefte für Chemie 128, 827–836 (1997)

Monatshefte für Chemie
Chemical Monthly

Surface Activity and Orientation of Inosine at a Mercury/Solution Interface

M. E. Ahmed

Chemistry Department, Faculty of Science, Assiut University, Assiut, Egypt

Summary. A systematic investigation on the adsorption and association of inosine at a hanging mercury drop electrode by phase-sensitive ac voltammetry has been performed. The adsorption equilibrium bas been determined as a function of various parameters such as *pH*, adsorption potential, adsorption time, and bulk concentration of inosine. It was found that the association of the adsorbed species depends predominantly on the stacking interactions of neutral inosine molecules. Over a wide potential range, inosine exhibits a dilute adsorption characteristic where it is adsorbed with the base flat on the electrode surface. Above a certain threshold value, inosine appears to undergo a surface reorientation and adopts a perpendicular position. The nucleation and growth mechanism is analyzed applying the *Avrami* equation. Characteristic properties and adsorption parameters of dilute and compact layers of inosine were evaluated from the two-step *Frumkin* isotherm and from the potential dependence of adsorption.

Keywords. Surface activity; Orientation; AC voltammetry; Inosine.

Oberflächenaktivität und Orientierung von Inosin an einer Quecksilber/Lösungs-Grenzfläche

Zusammenfassung. Die Adsorption und Assoziation von Inosin an einer Quecksilbertropfelektrode wurde mittels phasensensitiver AC-Voltammetrie systematisch untersucht. Die Abhängigkeit des Adsorptionsgleichgewichts von Parametern wie *pH*-Wert, Adsorptionspotential, Adsorptionszeit und Inosinkonzentration wurde gemessen. Dabei zeigte sich, daß die Assoziation der adsorbierten Spezies vorwiegend von der Anordnung und den Wechselwirkungen der neutralen Inosinmoleküle abhängt. Inosin bildet über einen weiten Potentialbereich eine dünne Adsorptionsschicht aus, wobei die Base flach auf der Elektrodenoberfläche aufliegt. Ab einem bestimmten Grenzwert der Konzentration tritt eine Reorientierung zu einer senkrechten Anordnung ein. Keimbildung und Wachstumsmechanismus wurden mittels der *Avrami*-Gleichung analysiert. Eigenschaften und Adsorptionsparameter der verdünnten und der kompakten Inosinschicht konnten aus der zweistufigen *Frumkin*-Isotherme und aus der Potentialabhängigkeit der Adsorption bestimmt werden.

Introduction

The surface activity of nucleic acid bases, nucleosides, and nucleotides at mercury/solution interfaces has been studied by various authors [1–13]. It has been shown that the adsorption of monomeric purine and pyrimidine derivatives results in a lowering of the differential capacitance of the electric double layer next to the

mercury electrode [1, 2]. At relatively low bulk concentrations of these substances, a rather dilute adsorption layer is established up to a certain threshold value, whereas a condensed film is formed above this concentration within a certain potential range [14]. In the potential region where the surface film is formed, a kind of a pit appears on the capacitance curves of ac polarograms [1, 2, 4, 8]. The forces which govern the formation of the intermolecular complexes in the film are of considerable interest not only from the theoretical point of view but also with respect to their significance for the stabilization of the structures of polynucleotides and polynucleotide-nucleotide complexes [6, 7]. The mechanism of this film formation has been analyzed quantitatively by *Retter* [15].

The present paper focuses on the investigation of surface activity and adsorption equilibria of inosine in a wide range of bulk concentration at different *pH* values and at different adsorption times. The adsorption parameters were also computed from the *Frumkin* double-step isotherm.

Results and Discussion

Phase-sensitive ac voltammograms of inosine in solutions of varying *pH* at the HMDE are shown in Fig. 1. The recorded capacitive ac component, in potential regions where no faradic process occurs, is proportional to the differential double layer capacitance [16]. Over the investigated *pH* range (2.0–12) and at low bulk concentrations, a progressive decrease of the capacitive ac signal is observed around the potential of maximum adsorption due to the surface activity and increasing adsorption of inosine at the electrode surface (Table 1). This decrease corresponds to the progressive coverage of the mercury electrode surface by a dilute adsorption layer (first stage of adsorption), and the process of adsorption leads to a decrease of the differential double layer capacity at the mercury/solution interface. At $5.2 < pH < 9.2$ and at more elevated bulk concentrations of inosine (above the threshold concentration value C_{th}, Table 1), a very clear capacitive pit is observed the width and depth of which depend on the *pH* and both increase with the bulk concentration of inosine (Fig. 1). The appearance of such a pit reflects the formation of a compact adsorption film (second adsorption stage) due to pronounced lateral interactions of adsorbed inosine species in a certain potential range. At potentials more negative than *ca.* -1.0 V, the ac voltammograms in presence of various concentrations of inosine are more or less identical to the ac voltammogram of the base electrolyte at various *pH* values. This behaviour reflects the very weak adsorption of inosine species at the negatively charged electrode surface due to the repulsion between the negatively charged surface and the π-electron system of the neutral inosine species and/or the negatively charged inosine species in alkaline solutions ($pK_{a2} = 8.8$).

The adsorption and association behaviour of inosine is similar to that of other purine nucleosides [12, 17]. For all of them, two adsorption stages can be resolved at the mercury electrode surface. In the first dilute stage, the nucleoside species are adsorbed parallel to the electrode surface forming a flat adsorption layer. In the second stage, however, the associated adsorbed species form a vertical stacked and compact adsorption layer at the mercury electrode surface. It should be mentioned that in alkaline solutions ($pH > 9.2$) the negative ionization of $-N_1H$ leads to

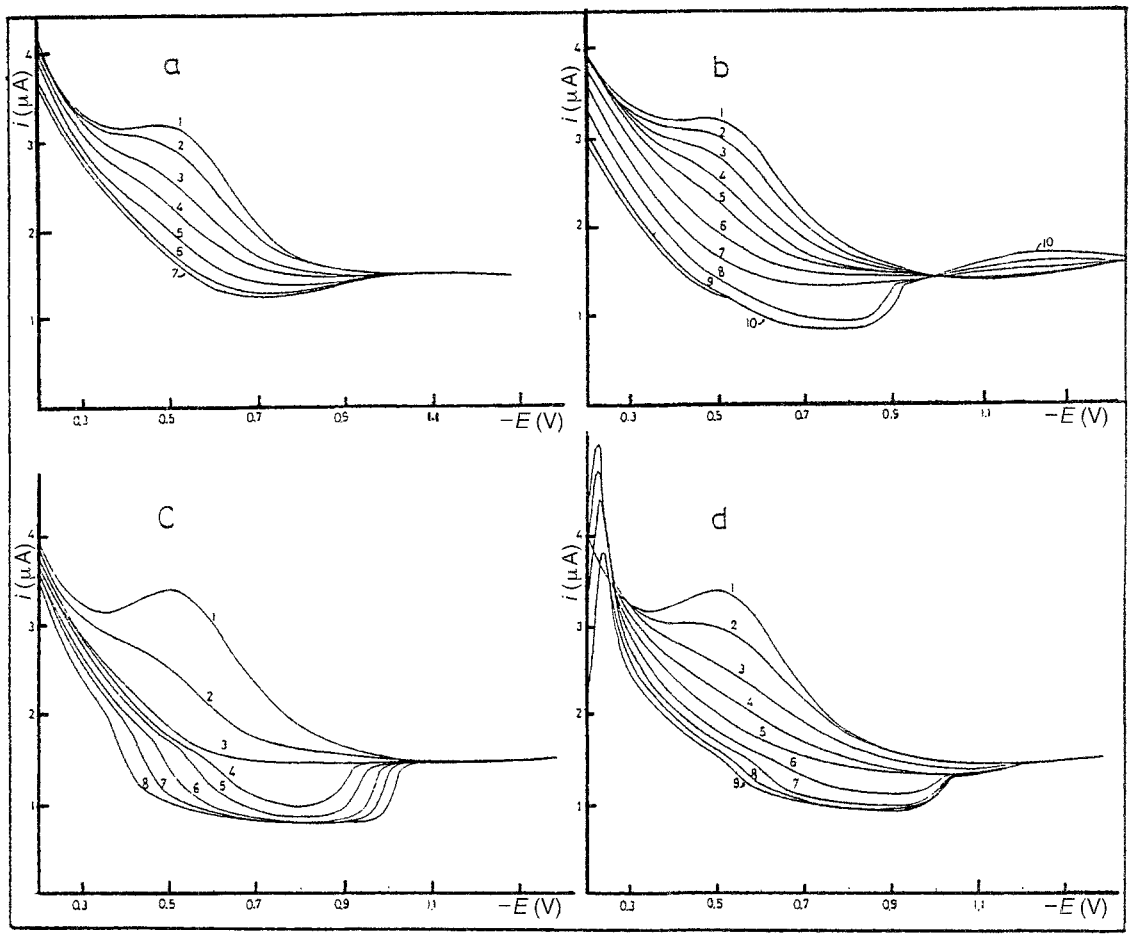

Fig. 1. AC capacitive current curves of inosine at *pH* (a) 3.2, (b) 5.2, (c) 7.2, and (d) 9.2; 0.5 *M Britton-Robinson* buffer (NaCl), 5°C, area of HMDE: 1.2 $\times 10^{-2}$ cm^2, scan rate: 5 mV·s^{-1}, amplitude: 10 mVpp, phase angle: 90°, frequency: 330 Hz, t_s: 60 s; (a): (1) 0.0, (2) 3.9, (3) 7.9, (4) 23.4, (5) 77.4, (6) 196.1, (7) 285.7 μ*M* inosine; (b): (1) 0.0, (2) 1.9, (3) 3.9, (4) 5.9, (5) 9.9, (6) 23.4, (7) 60.1, (8) 183, (9) 375, (10) 440 μ*M* inosine; (c): (1) 0.0, (2) 5.9, (3) 13.8, (4) 17.6, (5) 19.6, (6) 24.5, (7) 36.6, (8) 63.6 μ*M* inosine; (d): (1) 0.0, (2) 7.9, (3) 23.4, (4) 42.1, (5) 94.2, (6) 208, (7) 316, (8) 360, (9) 433 μ*M* inosine

Table 1. Adsorption parameters of dilute and compact layers of inosine at various *pH* values

pH	$-E$ (V)	C_{th} (mol/l)	a		β (l·mol^{-1})		$-\Delta G°$ (kJ·mol^{-1})	
			dilute	compact	dilute	campact	dilute	compact
5.2	0.75	16.0×10^{-5}	0.81	1.95	6.4×10^{4}	9.8×10^{2}	34.8	25.2
7.2	0.80	1.5×10^{-5}	0.82	2.05	2.7×10^{5}	7.9×10^{3}	38.2	30.0
9.2	0.85	16.0×10^{-5}	0.92	1.95	6.2×10^{4}	8.2×10^{2}	31.5	24.7

formation of the anionic form of inosine which inhibits the association phenomenon as well as the formation of the capacitance pit (second stage of adsorption). On the other hand, in acidic solutions ($pH < 5.2$) the extent of the pit diminishes, indicating that pit formation and degree of association of the adsorbed species are connected with the adsorption of neutral species of inosine. This is to be expected if the association of the adsorbed species depends mainly on the stacking interaction of the neutral molecules of inosine according to its pK values ($pK_{a1} = 1.2$, $pK_{a2} = 8.8$). Provided that the pit is formed due to association of perpendicularly oriented molecules, the reorientation from the planar and flat adsorption to the perpendicular one could be explained by an interaction of the electric field of the electrode with the permanent dipole of the neutral inosine molecule.

The formation of the first and second stage of adsorption can be followed from the capacitive current response (i_{ac}) on the adsorption time (t_s) at a constant mean electrode potential corresponding to the midle of the pit (Fig. 2). At the potential of maximum adsorption, the capacitive ac current slowly decreases (lines 2–5, Fig. 2) to an equilibrium value for low bulk concentrations of inosine. For concentrations larger than the threshold value characterized by occurrence of the pit, a drastic decrease to a second equilibrium value (lines 6–10, Fig. 2) is observed corresponding to the second stage of adsorption. The rearrangement of the surface layer from a dilute to a compact film stage manifested by the decrease of the out-of-phase ac current at bulk concentrations larger than the threshold concentration value is obviously a relatively slow process similar to crystallization. However, at very high bulk concentrations a large number of crystallization centers are formed at the electrode surface, and thus a compact layer is formed more rapidly. A similar phenomenon has been recorded for the formation of the compact layers of many purine ribosides [18] and pyrimidine ribosides [19].

The rates of nucleation and inosine film formation at the charged interface can be obtained using the *Avrami* plot [20] in the form of Eq. (1),

$$\ln(\ln(1/(1-\theta))) = m\ln t + \ln b \tag{1}$$

where m is characteristic for a given type of nucleation mechanism, b is related to the rate of nucleation and growth, t is the adsorption time, and θ is the degree of

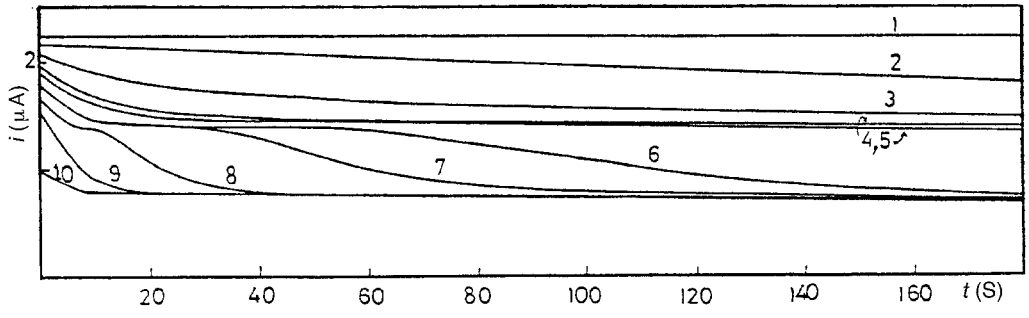

Fig. 2. Time dependence of the out-of-phase component of the ac current of inosine; *pH* 7.2, 0.5 *M Britton-Robinson* buffer (NaCl), $E_m = -0.75$ V, concentration of inosine: (1) 0.0, (2) 1.9, (3) 7.9, (4) 15.7, (5) 19.6, (6) 23.4, (7) 27.2, (8) 36.6, (9) 56.6, (10) 253.7 μ*M*; other conditions as in Fig. 1

coverage. The *Avrami* plots for capacitance transients of inosine (Fig. 3) indicate that the nucleation/growth process proceeds according to the *Avrami* theorem. Significant deviations can be observed near the pit edge where the rates of nucleation and growth are very low. Statistical estimates of m and b as a function of concentration were calculated by linear regression (Table 2). Values of either 2 or 3 were found for m corresponding to the two limiting cases of instantaneous and progressive nucleation, respectively.

Further quantitative studies on the adsorption and association of inosine at the mercury electrode surface could be elucidated by plotting Δi_{ac} (the decrease of i_{ac} with respect to i_{ac} of the base electrolyte for a given bulk concentration) as a

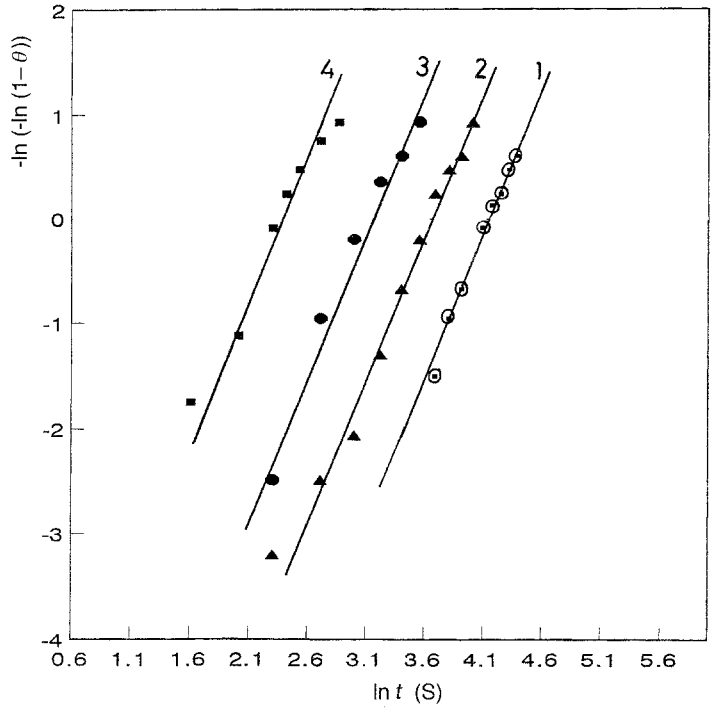

Fig. 3. *Avrami* plots for the short-time part of the capacitance *vs.* time transients at $E = -0.75$ V for different inosine concentrations; (1) 2.72×10^{-5}, (2) 3.10×10^{-5}, (3) 3.66×10^{-5}, (4) 4.58×10^{-5} mol·l^{-1}

Table 2. Parameters of the least-squares fit of the *Avrami* plot of transients for different Inosine concentrations at constant potential ($E = -0.75$ V) at *pH* 7.2 and 5°C

[Inosine] (mol·l^{-1})	m	$-\ln b$	r	s
2.72×10^{-5}	3.00	12.27	0.994	0.698
3.10×10^{-5}	2.676	8.40	0.987	1.152
3.66×10^{-5}	2.562	9.37	0.992	1.358
4.58×10^{-5}	2.308	5.50	0.986	0.922

function of the concentration of inosine. From the Δi_{ac} *vs.* C plot at the maximum adsorption potential at various *pH* values (Fig. 4), several interesting conclusions may be drawn. Two-step adsorption isotherm curves are obtained at different *pH* values (5.2–9.2), corresponding to the two adsorption stages of inosine at the electrode surface. The first stage reflects the flat adsorption stage for relatively low bulk concentrations of inosine. Above the threshold concentration value, the second stage adsorption can be seen, being due to strong lateral interaction and high interaction coefficients of adsorbed molecules and giving rise to a vertical stacked adsorption stage. It is concluded that at the maximum adsorption potential range the inosine molecule is oriented planar to the electrode surface when the interaction of the π-electron system of the molecule with the interface favors the adsorption. Above the threshold concentration value, the stacking interactions between the vertically oriented molecules lead to the formation of the second stage of adsorption, and the interaction of the electric field with the dipole moment of the molecule stabilizes the formation of the compact adsorption stage. This agrees well with the results of *Parsons* [21] and *Damaskin* [22] who found that the number of water molecules displaced from the interface by adsorption of hydrophobic organic species is doubled for a change in adsorption orientation from the planar to the vertical position. Figure 4 indicated also that the threshold concentration value at *pH* 5.2 and 9.2 is about 8–10 fold that of the value at *pH* 7.2. This behaviour

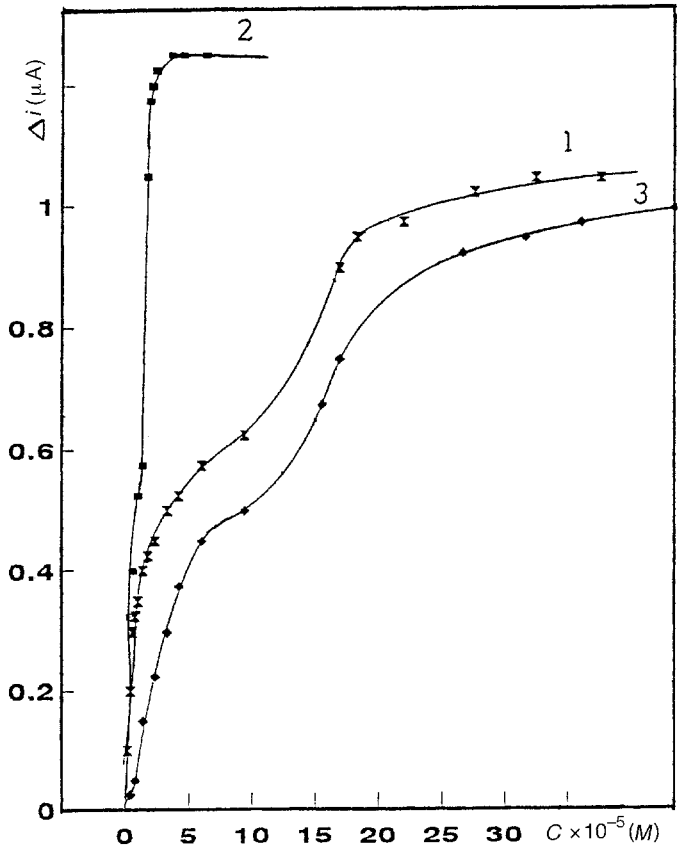

Fig. 4. Dependence of the capacity current decrease Δi_{ac} on the bulk concentration of inosine at *pH* (1) 5.2, (2) 7.2, and (3) 9.2 at the maximum adsorption potential; other conditions as in Fig. 1

supports the assumption that the association process of the adsorbed species at the electrode surface depends predominantly on the stacking of the neutral molecule of inosine.

In order to calculate the adsorption parameters of inosine at various *pH* values, the equilibrium values of the ac current at a given bulk concentration and at the maximal adsorption potential were measured, and the degree of coverage θ was calculated using Eq. (2),

$$\theta = C^\circ - C/C^\circ - C_m = \Delta i_{ac}/(\Delta i_{ac})_m \tag{2}$$

where C_i are the differential capacitances in the supporting electrolyte (C°), at a given bulk concentration of inosine (C), and at a bulk concentration corresponding to full coverage (C_m). Δi_{ac} is the decrease of the capacitive ac current (with respect to the i_{ac} of the base electrolyte) for a given bulk concentration, and $(\Delta i_{ac})_m$ is the maximal decrease corresponding to full coverage. It has been found that the experimental data can be approximately fitted to the *Frumkin* adsorption isotherm (Fig. 5) given by Eq. (3).

$$\beta \cdot C = (\theta/(1-\theta))\exp(-2a\theta) \tag{3}$$

θ is the degree of coverage, a is the interaction coefficient, β the adsorption coefficient, and C the bulk concentration of inosine; a was determined from the logarithmic plot of the *Frumkin* isotherm, and β from the value at half coverage ($\theta = 0.5$). The free energy of adsorption ΔG° could then calculated from Eq. (4).

$$\beta = (1/55.5)\exp(\Delta G^\circ/RT) \tag{4}$$

The value of the maximum surface concentration, Γ_m, was calculated using *Koryta*'s equation [23],

$$\Gamma_m = 0.736 \times 10^{-3} C \cdot (Dt)^{1/2} \tag{5}$$

where C is the bulk concentration of the inosine in $mol \cdot cm^{-3}$ and D the diffusion coefficient in $cm^2 \cdot s^{-1}$, which can be calculated using the *Stokes-Einstein* equation. The value of the maximum surface concentration Γ_m was obtained from Eq. (5) by taking the time as the extrapolated time at which the linearized first portion of the time dependence of the ac current reaches the final horizontal part, *i.e.* full coverage. The Γ_m value (4.38×10^{-10} mol·cm^{-2} at *pH* 7.2) indicates that the rather compact interfacial structure of the investigated compound favours an orientation of the bases perpendicular to the electrode surface. Nevertheless, the rather low average surface area ($S_m = 0.39\,nm^2$) for inosine in the compact film indicates a densely packed structure of the base residue of the compound oriented perpendicularly toward the surface of the electrode.

The adsorption parameters of inosine at various *pH* values for both the first and second stage of adsorption are summarized in Table 1. The values of a, β, and ΔG° for the first stage reflect the moderate lateral attractive interaction of adsorbed inosine molecules. For the second adsorption stage, the following tendencies emerge: The magnitude of β is significantly lower than that of the first stage. This significantly lower adsorptivity of the second stage correlates with its sensitivity to larger alteration of the adsorption potential and its tendency for sudden collapse at

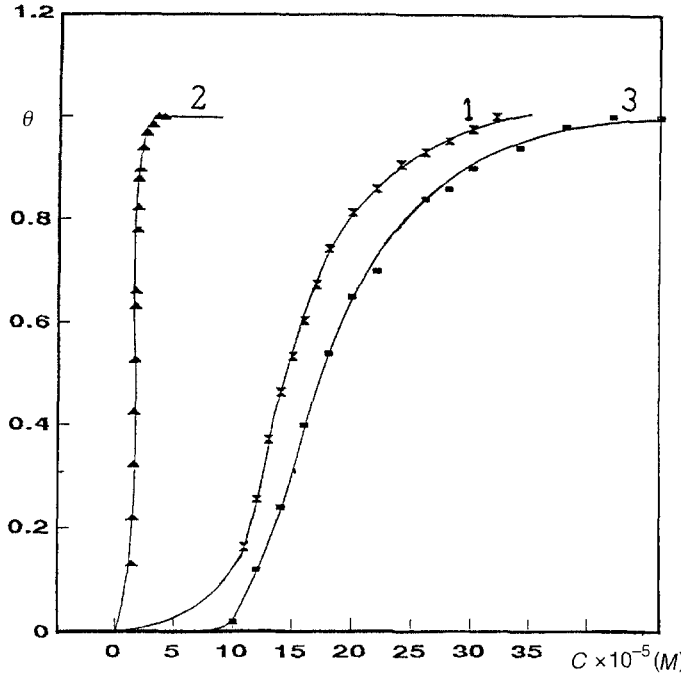

Fig. 5. Dependence of the surface coverage θ on the bulk concentration of inosine for a compact layer at *pH* (1) 5.2, (2) 7.2, and (3) 9.2; other conditions as in Fig. 1

a certain value of the interfacial electric field at the positive and the negative side of the region of maximal adsorption around the operative potential of zero charge. The interaction coefficient a generally increases in the second stage due to enhanced possibilities for intermolecular attractive interactions resulting from the perpendicular orientation and the greater population of the adsorbed molecules in the second stage of adsorption.

Comparison of the values of the adsorption parameters of inosine at different *pH* values (Table 1) shows a significant dependence on the H^+ concentration for both stages of adsorption. Surface activity and degree of association expressed by the value of β for both adsorption stages increases markedly at *pH* 7.2, a value at which the association and adsorbed molecules prevail in neutral form.

Comparison of the adsorption parameters of inosine with the corresponding data for guanosine (2-amino-inosine [17]) at the same *pH* shows that the surface activity of inosine in the dilute and compact stages is significantly smaller than that of guanosine. Thus, a bulk solution activity of about 15 μM is required to observe the surface orientation process (capacitance pit) for inosine, whereas an activity of 4.7 μM is required in the case of guanosine [17] (*pH* 7.2). This is a quantitative indication that the introduction of an electron releasing amino group into the inosine molecule increases the tendency for adsorption and stacking interactions between vertically oriented molecules [5]. It is remarkable that small steric

differences in the adsorbed molecules causing, for example, only a marginal change of pK_a values, yield a distinct change in the adsorption behaviour.

Experimental

Chemicals and solutions

Inosine was obtained from Sigma and was used without further purification. Solutions containing different concentrations of inosine were prepared by dissolving a known amount of the chemically pure product in an appropriate volume of *Britton-Robinson* buffer brought to a constant ionic strength of 0.5 *M* by the addition of NaCl and adjusted to the desired *pH*. All chemicals were of reagent grade. The *pH* was measured with a digital Radiometer *pH* meter, Model *pH M*64.

Apparatus and methods

A Princeton Applied Research (PAR) Model 174 polarographic analyser coupled with a PAR Model 174/50 ac polarographic interface and a PAR Model 510 (lock-in-amplifier) phase detector were employed for ac voltammetric measurements. Phase-sensitive ac voltammograms were recorded with a phase angle adjusted to 90°, corresponding to the out-of-phase component of the ac current (capacitive current component). The amplitude of the ac voltage was 10 mV peak-to-peak. The scan rate of the dc ramp of the mean electrode potential E was 2 $mV \cdot s^{-1}$, and the ac frequency had a value of 330 Hz unless stated otherwise. The time dependence of the ac component of the capacitive current at an adjusted constant mean electrode potential E was obtained as described earlier [12].

A thermostatted PAR cell equipped with a three-electrode system was used for the voltammetric studies. The three-electrode system contained a HMDE as the working electrode, an Ag/AgClsat.-KCl reference electrode, and a platinum wire counter electrode. The solution was degassed with pure nitrogen before the performance of electrochemical experiments.

References

[1] Vetterl V (1966) Collect Czech Chem Commun **31**: 2105
[2] Vetterl V (1968) J Electroanal Chem **19**: 169
[3] Janik B, Elving BJ (1968) Chem Rev **68**: 295
[4] Brabec V, Christian SD, Kim MH, Dryhurst G (1977) J Electroanal Chem **85**: 389
[5] Baker JG, Christian SD, Kim MH, Dryhurst G (1979) Biophys Chem **9**: 355
[6] Krznaric D, Valenta P, Nurnberg HW (1975) J Electroanal Chem **65**: 863
[7] Valenta P, Nurnberg HW, Krznaric D (1976) Bioelectrochem Bioenerg **3**: 418
[8] Vetterl V, Kovarikova E, Zaludova R (1977) Bioelectrochem Bioenerg **4**: 389
[9] Temerk YM, Valenta P (1978) J Electroanal Chem **93**: 57
[10] Temerk YM (1979) Can J Chem **57**: 1136
[11] Vetterl V, Pokorny J (1980) Bioelectrochem Bioenerg **7**: 517
[12] Temerk YM, Kamal MM (1983) Bioelectrochem Bioenerg **11**: 457
[13] Kamal MM, Temerk YM, Ahmed ME, Ahmed ZA (1986) Bioelectrochem Bioenerg **16**: 485
[14] Retter U, Vetterl V, Jehring H (1974) J Electroanal Chem **57**: 391
[15] Retter U (1978) J Electroanal Chem **87**: 181
[16] Jehring H (1974) Elektrosorptionsanalyse mit der Wechselstrompolarographie. Akademie Verlag, Berlin
[17] Temerk YM, Kamal MM (1981) Bioelectrochem Bioenerg **8**: 671

[18] Ahmed ZA, Ahmed ME, Ibrahim MS, Kamal MM, Temerk YM (1994) Anal Chim Acta **289**: 329
[19] Kamal MM, Temerk YM, Ahmed ZA, Ibrahim MS (1990) Bioelectrochem Bioenerg **24**: 165
[20] Avrami M (1939) J Chem Phys **7**: 1103
[21] Parry JM, Parasons R (1966) J Electroanal Soc **113**: 992
[22] Damaskin BB, Dyatkina SL, Petrochenko SL (1969) Elektrokhimiya **5**: 935
[23] Koryta J (1953) Collect Czech Chem Commun **18**: 206

Received January 7, 1997. Accepted (revised) March 24, 1997